

Long-lived spin entanglement induced by a spatially correlated thermal bath

D. P. S. McCutcheon,^{1,2,*} A. Nazir,¹ S. Bose,¹ and A. J. Fisher^{1,2}

¹*Department of Physics and Astronomy, University College London,
Gower Street, London WC1E 6BT, United Kingdom*

²*London Centre for Nanotechnology, University College London*

(Dated: September 1, 2009)

We investigate how two spatially separated qubits coupled to a common heat bath can be entangled by purely dissipative dynamics. We identify a new dynamical timescale associated with the lifetime of the dissipatively-generated entanglement and show that it can be much longer than either the typical single-qubit decoherence time, or the timescale on which a direct exchange interaction can entangle the qubits. We give an approximate analytic expression for the long-time evolution of the qubit concurrence and propose an ion trap scheme in which such dynamics should be observable.

PACS numbers: 03.67.Bg, 03.65.Yz, 03.67.Pp

I. INTRODUCTION

Entanglement is the hallmark of correlations in quantum theory and has come to be seen as a precious resource essential for many quantum information processing protocols [1]. An entangled state can show correlations stronger than those allowed classically, however, these correlations are often extremely fragile. Interactions with the environment surrounding any quantum system tend to cause a rapid loss of quantum coherence [2], generally leading to entanglement within the system being destroyed on a short timescale [3]. Various techniques have thus been developed to protect entangled states from their surroundings, such as constructing decoherence free subspaces [4, 5], dynamical decoupling [6, 7], and exploiting the quantum Zeno effect [8].

As well as avoiding decoherence, entanglement must also be generated. This can be achieved by a number of means; for example, by harnessing intrinsic system couplings [9], through projective measurements [10], or via a quantum bus [11]. Recently, it was shown that entanglement between a pair of two-level systems (qubits) can in fact be generated by the same processes that are usually considered to be detrimental, if the qubits are allowed to interact with a common bath [12, 13]. This offers a potential way to explore the interplay between coherent and incoherent multi-qubit dynamics with a significantly reduced level of external system control.

In general, immersing a pair of otherwise non-interacting spins in a common heat bath will give rise to two terms in the subsequent master equation: a unitary, Hamiltonian-like Lamb-shift term [2, 14] leading to coherent spin evolution, and a dissipative term [2, 13], both of which may generate spin entanglement [12, 13, 14, 15, 16]. While it is known that in the idealised case of unseparated qubits entanglement induced by the *dissipative* term can persist indefinitely [17], surprisingly little

attention has been paid to the dynamics of its generation and decay in the more realistic setting of *finite* inter-qubit separation. In this experimentally relevant case, it is not clear on what timescale the generated entanglement persists, or even whether its observation is feasible at all. It has been shown that the entangling capability of the Lamb-shift is highly sensitive to the inter-qubit separation [14], with dissipative processes destroying any generated entanglement more rapidly as separation increases. Furthermore, it has recently been shown that the level of entanglement generated between two harmonic oscillators suffers from a similar critical dependence on oscillator separation [18]. Hence, a comparison of the timescales associated with conventional decoherence dynamics to those for dissipatively-induced spin-entanglement generation and decay is needed.

In this article, we address the above issues by studying the dynamics of bath-induced entanglement in the context of the two-spin-boson model, which has wide applications in the solid state and elsewhere [19, 20]. We show that for small but finite spin separation, the timescale on which dissipatively-induced spin entanglement survives can be far larger than the corresponding single spin decoherence time. It also exceeds the timescale on which entanglement induced by either a *direct exchange interaction* or the Lamb-shift persists. In particular, we obtain an approximate analytic expression for the long-time dynamics of the two-spin concurrence and from this determine its survival time. We suggest an ion trap realisation of our model and demonstrate that observation of the generated entanglement should indeed be feasible.

II. MASTER EQUATION

We consider two spatially separated, identical, non-interacting spin qubits, each subject to a static field of strength $\Delta/2$ in the x -direction, and coupled to a common bath of harmonic oscillators. The Hamiltonian is

*Electronic address: dara.mccutcheon@ucl.ac.uk

given by

$$H = H_S + H_I + H_B$$

$$= -\frac{\Delta}{2} \sum_{n=1}^2 \sigma_x^n + \sum_{n=1}^2 \sigma_z^n \otimes B_n + \sum_k \omega_k b_k^\dagger b_k, \quad (1)$$

with $\hbar = 1$. Here, σ_i^n is a Pauli operator acting on the n th qubit ($n = 1, 2$; $i = x, y, z$), B_n is the bath operator coupling qubit n to the bath, while ω_k is the angular frequency, and b_k^\dagger (b_k) the creation (annihilation) operator of the bath mode of wave vector k .

To investigate the dynamics of the reduced two-spin density operator ρ we assume that the qubit-bath coupling is weak compared to Δ and follow the standard Born-Markov and rotating-wave approximation approach [2]. This relies on a perturbative expansion in the system-bath coupling strength, and the assumption that the bath instantly re-thermalises after any interaction with the qubits. Setting $\langle H_I \rangle_B = 0$, we obtain a Schrödinger-picture master equation of the usual form

$$\frac{d\rho(t)}{dt} = -i[H_S + H_{LS}, \rho(t)] + \mathcal{D}(\rho(t)), \quad (2)$$

valid to second order in H_I . Here, the Lamb-shift provides a Hamiltonian-like contribution and is of the form

$$H_{LS} = A(\sigma_x^1 + \sigma_x^2) + B(\sigma_z^1 \sigma_z^2 + \sigma_y^1 \sigma_y^2), \quad (3)$$

where we have omitted a constant. The precise expressions for A and B depend on the details of the qubit-bath interactions and will be given in section III. For now we will comment on their likely qualitative effects. The first term of H_{LS} simply renormalises the static field strength due to the presence of the bath modes. The entangling capability of the second term deserves some attention since it represents an induced interaction between the two qubits, as has been explored in detail in Ref. [14]. However, we will show that in general this entanglement decays at a rate far quicker than that generated by the dissipator, here given by

$$\mathcal{D}(\rho(t)) = \sum_{\omega} \sum_{n,m=1}^2 \gamma_{nm}(\omega) (A_m(\omega) \rho(t) A_n^\dagger(\omega) - \frac{1}{2} \{A_n^\dagger(\omega) A_m(\omega), \rho(t)\}), \quad (4)$$

with frequency summation over the eigenvalue differences of H_S ($\omega = \pm\Delta$) and corresponding eigenoperators $A_n(\pm\Delta) = (1/2)(\sigma_z^n \mp i\sigma_y^n)$.

III. BATH CORRELATION FUNCTIONS

The key quantities in the present discussion are the Fourier transforms of the bath correlation functions $\gamma_{nm}(\omega) = \int_{-\infty}^{\infty} ds e^{i\omega s} \langle B_n^\dagger(s) B_m \rangle$, for which we need a specific form for B_n . As usual in the spin-boson model,

we consider linear coupling between the qubits and the coordinate of each bath mode [19, 20, 21], such that $B_n(s) = \sum_k (g_k^n b_k^\dagger e^{i\omega_k s} + g_k^{n*} b_k e^{-i\omega_k s})$, with coupling constants g_k^n . Note that with this form of B_n our assumption of $\langle H_I \rangle_B = 0$ leading to Eq. (2) is justified. An important aspect of this work is that the qubits have an explicit spatial separation and thus $g_k^1 \neq g_k^2$. To make this evident, we consider our spins to be separated by a distance d along the z -axis such that $g_k^1 = g_k e^{idk \cos \theta/2}$ and $g_k^2 = g_k e^{-idk \cos \theta/2}$, where θ is the polar angle measured against the z -axis in k -space, and $|g_k^1| = |g_k^2| = g_k$. Taking the bath to be in thermal equilibrium, we find

$$\gamma_{12}(\omega) = \int_{-\infty}^{\infty} ds e^{i\omega s} \sum_k |g_k|^2 (N(\omega_k) e^{i\omega_k s} e^{ikd \cos \theta} + (N(\omega_k) + 1) e^{-i\omega_k s} e^{-ikd \cos \theta}), \quad (5)$$

where $N(\omega_k) = [\exp(\omega_k/k_B T_B) - 1]^{-1}$ is the thermal occupation of mode k , k_B is Boltzmann's constant, T_B the temperature of the bath, $\gamma_{12}(\omega) = \gamma_{21}(\omega)$ (once the summation is performed), and $\gamma_{nn}(\omega)$ is obtained by setting $d = 0$.

Defining the bath spectral density to be $J(\omega) = \sum_k |g_k|^2 \delta(\omega - \omega_k)$ [19], and an inverse dispersion relation (assumed isotropic) $k = \kappa(\omega)$, we take the continuum limit of the summation over k above to find

$$\gamma_{12}(\omega) = f(\kappa(\omega)d) \gamma_{11}(\omega), \quad (6)$$

with $\gamma_{11}(+\Delta) = \gamma_{22}(+\Delta) = (N(\Delta) + 1)\gamma_0$ and $\gamma_{11}(-\Delta) = \gamma_{22}(-\Delta) = N(\Delta)\gamma_0$, where $\gamma_0 = 2\pi J(\Delta)$ is the single-spin decoherence rate at zero temperature. Here, $f(x)$ describes the bath's spatial correlations and is determined by its dimensionality $D (= 1, 2, 3)$. For $D = 1$ we have $f(x) = \cos(x)$; for $D = 2$, $f(x) = J_0(x)$, where J_0 is a Bessel function of the first kind; and for $D = 3$, $f(x) = \text{sinc}(x)$. We thus write

$$\gamma_{12}(\pm\Delta) = (1 - \delta) \gamma_{11}(\pm\Delta), \quad (7)$$

where $1 - \delta$ captures the degree of correlation between the baths seen by each qubit, becoming unity at $d = \delta = 0$ (completely correlated) and, for $D > 1$, zero as $d \rightarrow \infty$ ($\delta \rightarrow 1$, completely independent). When $D = 1$, the Markovian assumption constrains γ_{12} to be periodic with respect to d . However, we will concentrate here on the limit where d is small enough such that $\delta \approx (\kappa(\Delta)d)^2/2D$, for all D .

The strength of the two terms in the Lamb-shift Hamiltonian are given by combinations of the Hilbert transforms of the bath correlation functions. They are found to be

$$A = 2 \int_0^\infty J(\omega) \coth(\omega/(2k_B T_B)) \left(\frac{\Delta}{\Delta^2 - \omega^2} \right) d\omega \quad (8)$$

and

$$B = \int_0^\infty J(\omega) f(\kappa(\omega)d) \left(\frac{\omega}{\Delta^2 - \omega^2} \right) d\omega \quad (9)$$

where principal values are assumed. Note that for system-bath coupling in 2 or 3 dimensions $B \rightarrow 0$ as the qubit separation is increased to infinity, expressing the fact that an uncorrelated bath can not give rise to any coherent coupling between the qubits. In contrast, A contains no distance dependence since it represents a renormalisation of the single-qubit energy levels in each spin, independent of any bath correlations.

The relative strength of the coherent terms in the evolution, A and B , compared to the strength of the dissipative terms, given by γ_{11} and γ_{12} , dictates whether the bath is capable of generating entanglement through the Lamb-shift [14]. Evaluation of the relevant integrals involved necessitates a specific form of the bath spectral density. In this article we shall focus on the entanglement generated through dissipative processes and as such we may leave A and B unevaluated. In fact, we shall show in Section VI that the dissipatively induced entanglement can persist for times far larger than entanglement generated through the Lamb-shift, regardless of its strength.

IV. STATE DYNAMICS

Rather than working directly with the reduced density operator ρ , it is more instructive to work in terms of a 16 dimensional vector α , which is a generalisation of the Bloch vector for two-qubit states. It is constructed by flattening the matrix whose elements α_{ij} satisfy

$$\rho = \frac{1}{4} \sum_{i,j=0}^3 \alpha_{ij} \sigma_i^1 \otimes \sigma_j^2, \quad (10)$$

where $\sigma_0^1 = \sigma_0^2 = I$. The traceless property of the Pauli matrices ensures that $\alpha_{ij} = \langle \sigma_i^1 \sigma_j^2 \rangle$, and conservation of probability demands that $\alpha_{00} = 1$. To describe the evolution of our system, we consider the eigensystem of the Liouvillian super-operator \mathcal{L} defined (unconventionally) by $\dot{\alpha}(t) = \mathcal{L}\alpha(t)$, where the linearity of the transformation between ρ and α ensures that the dynamics generated by \mathcal{L} is equivalent to that of Eq. (2). Clearly, a state α initially in an eigenstate of \mathcal{L} , say α_l (with eigenvalue λ_l), will evolve according to $\alpha(t) = \alpha_l e^{\lambda_l t}$. Hence, a general state evolves such that

$$\alpha(t) = \sum_{l=0}^{15} a_l \alpha_l e^{\lambda_l t}, \quad (11)$$

where the coefficients a_l are determined from the initial conditions, and the sum runs over all eigenstates of \mathcal{L} .

We are primarily interested in the long-time dynamics of our system. Hence, it makes sense to search for eigenvalues of \mathcal{L} with small (or zero) real parts since, assuming these parts are all negative, the corresponding eigenvectors will contribute towards the total state Eq. (11) on the largest timescale. We evaluate the full eigensystem of \mathcal{L} analytically, though this leads to cumbersome expressions which we shall not give here. However, we can identify a number of important features for our subsequent

analysis. For any non-zero qubit separation ($\delta \neq 0$) there exists a single eigenvector, α_0 , with zero eigenvalue, and all other eigenvalues have negative real parts. We therefore associate α_0 with the thermal state since it is that to which all states tend towards as $t \rightarrow \infty$. Of the remaining 15, there is a single eigenvalue, λ_1 (with corresponding eigenvector α_1), which vanishes as $\delta \rightarrow 0$ at all temperatures. Expanding the exact expression to first order in δ and second order in $N(\Delta)$ gives the simple form

$$\lambda_1 = -(1 + 3N(\Delta))\delta\gamma_0. \quad (12)$$

It is also possible to show graphically that λ_1 varies approximately linearly with $N(\Delta)$ at all temperatures. For reasons that should become clear, we shall refer to the eigenvector corresponding to the null eigenvalue, α_0 , and the eigenvector corresponding to the vanishing eigenvalue, α_1 , as our eigenvectors of interest. The eigenvector corresponding to the thermal state, α_0 , is expressible solely in terms of $R = (1 + 2N(\Delta))^{-1} = \tanh(\Delta/2k_B T_B)$, and is given by

$$\alpha_0 : \{\alpha_{00}, \alpha_{01}, \alpha_{11}, \alpha_{22}\} = \{1, R, R^2, 0\}, \quad (13)$$

where the notation implies that the eigenvector has the elements specified, and that $\alpha_{22} = \alpha_{33}$, $\alpha_{01} = \alpha_{10}$, with all other elements being zero. From a numerical analysis of α_1 we find that for $\delta \ll 1$, to a very good approximation α_1 can also be expressed just in terms of R , with corrections being of the order of δ :

$$\alpha_1 : \{\alpha_{00}, \alpha_{01}, \alpha_{11}, \alpha_{22}\} \approx \{0, R, 1 + R^2, 1\}, \quad (14)$$

where the notation is the same as in Eq. (13).

There are two further notable eigenvalues, λ_2 and $\lambda_3 = \lambda_2^*$. Once again, expanding the exact eigenvalues to first order in δ , and to first order in R about $R = 1$, gives the expression

$$\lambda_2 = \lambda_3^* = -(1/2)\gamma_0(1 - R + 2\delta - \delta R) - i\Delta. \quad (15)$$

Note that these eigenvalues have vanishing real parts only in the limit that both the separation and temperature go to zero ($\delta \rightarrow 0$ and $R \rightarrow 1$). In either the zero temperature limit ($R \rightarrow 1$) or the zero separation limit ($\delta \rightarrow 0$) the corresponding eigenvectors, α_2 and $\alpha_3 = \alpha_2^*$, are given by

$$\alpha_2 : \{\alpha_{02}, \alpha_{03}, \alpha_{12}, \alpha_{13}\} = \{i, 1, i, 1\}, \quad (16)$$

where once again the notation implies the eigenvector has the elements specified but this time with $\alpha_{20} = -\alpha_{02}$, $\alpha_{30} = -\alpha_{03}$, $\alpha_{21} = -\alpha_{12}$ and $\alpha_{31} = -\alpha_{13}$, and all other elements being zero.

This leaves us with 12 eigenvalues to consider. Plotting their real parts as a function of R it becomes clear that they are all $\sim -\gamma_0/R$, for all values of δ . As such, the corresponding eigenvectors contribute towards the total state significantly only for times $t < \gamma_0^{-1}$ regardless of the temperature. These eigenvalues and eigenvectors shall be referred to as those with $l > 3$.

With the relative size of the real parts of the various eigenvalues in mind, we see that for small enough δ , at times sufficiently greater than γ_0^{-1} , a general state can be approximated by

$$\alpha(t) = \alpha_0 + a_1 \alpha_1 e^{\lambda_1 t} + a_2 (\alpha_2 e^{\lambda_2 t} \pm \alpha_2^* e^{\lambda_2^* t}), \quad (17)$$

where we have normalised α_0 , set $a_0 = 1$, and set $a_3 = \pm a_2$ to ensure positivity of the corresponding density operator. The coefficient a_1 is found, by setting $t = 0$ in Eq. (11), to be $a_1 = (\Lambda - R^2)/(3 + R^2)$, where $\Lambda = \langle \sigma^1 \cdot \sigma^2 \rangle = \alpha_{11} + \alpha_{22} + \alpha_{33}$. For separable pure states Λ represents a scalar product of single qubit Bloch vectors. Positivity of the corresponding density operator limits the range of Λ to $-3 \leq \Lambda \leq +1$.

To gain insight into the general features of a state described by Eq. (17), it is useful to write down the corresponding density operator in the zero temperature and separation limit, in which there are no decoherent processes due to the real parts of the relevant eigenvalues vanishing. Using Eq. (10) we find

$$\begin{aligned} \rho(t) = & (1 + a_1) |\uparrow\uparrow\rangle_x \langle\uparrow\uparrow|_x - a_1 |\Psi^-\rangle_x \langle\Psi^-|_x \\ & + a_2 \sqrt{2} \left(e^{-i\Delta t} |\Psi^-\rangle_x \langle\uparrow\uparrow|_x \pm e^{i\Delta t} |\uparrow\uparrow\rangle_x \langle\Psi^-|_x \right), \end{aligned} \quad (18)$$

where $|\Psi^-\rangle_x = (1/\sqrt{2})(|\uparrow\downarrow\rangle_x - |\downarrow\uparrow\rangle_x) = (1/\sqrt{2})(|\uparrow\downarrow\rangle_z - |\downarrow\uparrow\rangle_z)$ is the Bell singlet, and $|\uparrow\uparrow\rangle_x = (1/2)(|\uparrow\uparrow\rangle_z + |\downarrow\downarrow\rangle_z + |\uparrow\downarrow\rangle_z + |\downarrow\uparrow\rangle_z)$. The subscripts x and z refer to the relevant basis, with our qubits defined with respect to z . Written in this way, we can see that our state is a coherent mixture of the singlet and the state $|\uparrow\uparrow\rangle_x$. At zero temperature, the state $|\uparrow\uparrow\rangle_x$ is the ground state since it minimises the energy associated with the system Hamiltonian and energy can not be absorbed from the environment. Also, at zero separation, the Bell singlet is stable since it is the totally anti-symmetric state, while the Hamiltonian is totally symmetric [22]. Therefore, in a combination of these limits coherent mixtures of these states are stable. However, the states are at different energies which gives rise to the exponential factors in Eq. (18).

V. ENTANGLEMENT DYNAMICS

We are now in a position to say that, provided our qubits are sufficiently close together such that $\delta \ll 1$, for times $t > \gamma_0^{-1}$ contributions from eigenvectors with $l > 3$ and their associated dynamics will have all but vanished, and to a good approximation (and a better approximation as time increases), our two-qubit state will be well described by Eq. (17). To quantify the resulting entanglement dynamics we use Wootters concurrence [23], which ranges from 0 for separable states to 1 for maximally entangled states. It can be shown numerically that the concurrence of a state described by Eq. (17) depends only

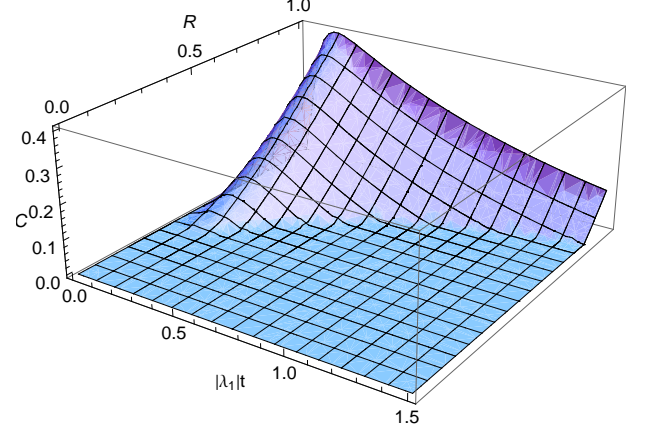


FIG. 1: (Color Online) Concurrence of the initially separable state $|\uparrow\downarrow\rangle$ in either x , y , or z ($\Lambda = -1$) as a function of time (scaled by λ_1) and $R = \tanh(\Delta/2k_B T_B)$ calculated from the full Liouvillian, though ignoring the Lamb-shift.

very weakly on the magnitude of a_2 , and in the zero temperature and separation limit has completely vanishing dependence. We may therefore set $a_2 = 0$ to derive a simple concurrence expression, and from Eqs. (13), (14) and (17) find

$$C = \max \left[\frac{(R^2 - 1)(R^2 + 3) + (R^2 - \Lambda)(3 - R^2)e^{\lambda_1 t}}{2(R^2 + 3)}, 0 \right], \quad (19)$$

valid (with increasing accuracy) for timescales $t > \gamma_0^{-1}$. The legitimacy of setting $a_2 = 0$ will be demonstrated towards the end of this section, where comparisons with numerics using the full eigensystem of \mathcal{L} are made.

Whether the bath is capable of inducing spin entanglement, and if so how it subsequently decays, is now clear. Firstly, no entanglement is generated unless

$$\Lambda < \frac{5R^2 - 3}{3 - R^2}, \quad (20)$$

in agreement with Ref. [17]. Secondly, provided this inequality is satisfied, we see from Eq. (19) that the induced entanglement will decay exponentially until $(R^2 - \Lambda)(3 - R^2)e^{\lambda_1 t} = -(R^2 - 1)(R^2 + 3)$ is satisfied, after which time the entanglement is zero. This occurs at

$$t_c = \frac{1}{|\lambda_1|} \ln \left[\frac{(R^2 - \Lambda)(R^2 - 3)}{(R^2 + 3)(R^2 - 1)} \right], \quad (21)$$

as demonstrated in Fig. 1. Note that Eqs. (19) and (21) are valid for a range of temperatures, however, in view of the inequality of Eq. (20), we will focus on small temperatures since these maximise the amount and lifetime of any induced entanglement. Interestingly, in the limit of vanishing temperature ($R \rightarrow 1$), the entanglement reaches zero only asymptotically. Also, as the qubit

separation $d \rightarrow 0$ the level of entanglement becomes a function of the initial state only and $t_c \rightarrow \infty$, i.e. the steady-state becomes entangled [17]. In general, t_c varies as $(\delta\gamma_0)^{-1}$ for given R and Λ , hence it can be lengthened by increasing the ratio Δ/T_B , or by decreasing the separation d .

We would naturally like to know which initially separable states result in the largest generated concurrence. For fixed temperature and spin separation the only parameter to consider is Λ , and from inspection of Eq. (19) we see that it should be minimised. This corresponds to an initial state that is as anti-symmetric as possible; hence, Λ is minimised by anti-aligning the single spin Bloch vectors, giving $\Lambda = -1$ for pure states. Such a state corresponds to $|\uparrow\downarrow\rangle$ in x , y or z . As the states become more mixed, the Bloch vectors decrease in length and $\Lambda \rightarrow 0$. Interestingly, even a *maximally mixed state* ($\Lambda = 0$) can become entangled provided $\Delta > 2 \coth^{-1}(\sqrt{5/3})k_B T_B$. In general, we expect an initially separable state to reach its maximum entanglement after a time $\sim \gamma_0^{-1}$, typical of the decay of eigenvectors α_l for $l > 3$. Note that if we do not restrict our initial state to a separable state, Λ is minimised by the Bell singlet, for which $\Lambda = -3$. As we have mentioned, in the limit that the qubit separation goes to zero the singlet is able to maintain its full entanglement for all times.

To illustrate these points, in the main part of Fig. (2) we plot the time evolution of the concurrence for various initial states, calculated both from Eq. (19) (dashed lines) and numerically using the full Liouvillian (solid lines), though here ignoring the Lamb-shift. As claimed, on timescales $> \gamma_0^{-1} \sim \delta$ in the scaled time units, the entanglement dynamics is well approximated by the analytic form. Note also that neglecting the eigenvectors α_2 and α_3 has had no discernible effect on the accuracy of Eq. (19) on the timescales it is expected to be valid. For the initially separable states ($\Lambda = -1, 0$), we clearly see that the entanglement reaches its maximum on a timescale $> \gamma_0^{-1} \sim \delta$, decaying subsequently at a rate $\sim \delta\gamma_0$. For the Bell singlet ($\Lambda = -3$), the analytic approximation becomes almost exact since this state is simply a linear combination of the vectors α_0 and α_1 in Eqs. (13) and (14). Also shown is the behaviour of the Bell state $(1/\sqrt{2})(|\uparrow\downarrow\rangle_z + |\downarrow\uparrow\rangle_z)$, for which $\Lambda = 1$. Unlike the singlet, all other Bell states have the maximum possible value of Λ , and as such lose their entanglement rapidly.

We could consider the maximally mixed state ($\Lambda = 0$) as being the infinite temperature thermal state since it represents a state for which thermal fluctuations completely overcome any external fields. We see that as the bath “cools” this state towards the thermal state at T_B , it does so via entangled states. Of course, after a time t_c the state of the qubits becomes separable once more, and will eventually reach the thermal state at T_B . There is in fact a well defined condition for T_B and (initially prepared) qubit temperature T_Q such that the bath has the ability to entangle the qubits. In the

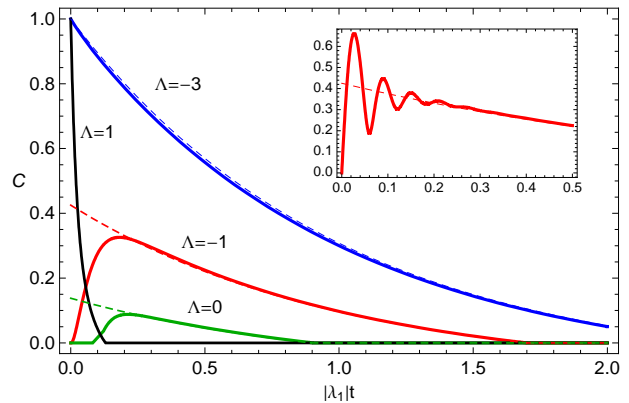


FIG. 2: (Color Online) Main: Concurrence as a function of (scaled) time calculated analytically (dashed lines, valid for $t > \gamma_0^{-1}$) and numerically (solid lines). We consider four initial states, the Bell singlet $(1/\sqrt{2})(|\uparrow\downarrow\rangle - |\downarrow\uparrow\rangle)$ (blue, $\Lambda = -3$), the pure state $|\uparrow\downarrow\rangle$ (red, $\Lambda = -1$), the maximally mixed state $\rho = (1/4)I$ (green, $\Lambda = 0$) and the Bell state $(1/\sqrt{2})(|\uparrow\downarrow\rangle + |\downarrow\uparrow\rangle)$ (black, $\Lambda = 1$). Parameters: $\delta = 0.05$, $R = 0.9$. Inset: Behaviour of the initial state $|\uparrow\downarrow\rangle$ where, in the numerical calculations, the Lamb-shift and exchange interactions have been included at an arbitrarily chosen strength $B = \xi = 1/(2|\lambda_1|)$.

limit of small bath and qubit temperature this condition becomes $\theta_B - \theta_Q > \frac{1}{2}\ln 3$, where $\theta_B = (\Delta/2k_B T_B)$ and $\theta_Q = (\Delta/2k_B T_Q)$.

VI. ENTANGLEMENT GENERATED THROUGH THE LAMB-SHIFT

It is important to consider the role of the Lamb-shift Hamiltonian H_{LS} , thus far ignored. Within the limits of our derivation, namely that Δ is large and hence rotations about x are so rapid that the y - and z - directions are effectively equivalent, its form is determined by symmetry. With this form it commutes with our eigenvectors of most interest, α_0 and α_1 . It can also be shown that the eigenvectors α_2 and α_3 are eigenoperators of H_{LS} , with eigenvalues $2(A+B)$ and $-2(A+B)$, respectively. Therefore, the Lamb-shift Hamiltonian can influence only the eigenvectors with $l > 3$, the imaginary parts of their eigenvalues, and the imaginary parts of λ_2 and λ_3 . Hence, despite the fact that H_{LS} can entangle our spins, its effect is restricted to a timescale of order γ_0^{-1} (after which the other eigenvectors have decayed) regardless of its amplitude, and it will therefore have no effect on the long-time entanglement dynamics or the analytic expressions we have derived.

In fact, we can further account for the effect of a direct spin exchange interaction simply by adding a term of the form $H_E = \xi \sigma^1 \cdot \sigma^2$ into H_S in Eq. (2), provided that the evolution it generates occurs on timescales much slower than the bath correlation time. This procedure is valid

in the regime of $\Delta \gg \xi$, such that Δ sets the relevant frequency scale for the system-bath interaction. In this case, exactly the same conclusions hold as for the Lamb-shift term since α_0 and α_1 again commute with this form of interaction, and α_2 and α_3 are also eigenoperators of H_E . Its influence will thus similarly be restricted to short timescales $\sim \gamma_0^{-1}$. This point is illustrated in the inset of Fig. (2) where we plot the analytically and numerically calculated concurrence of the initial state $|\uparrow\downarrow\rangle$ in x , y or z , including both H_{LS} and H_E with arbitrarily chosen strengths. As expected, their impact is seen only on a timescale $\sim \gamma_0^{-1}$, much shorter than that over which the dissipatively induced entanglement survives.

VII. EXPERIMENTAL REALISATION

While spin-boson models apply commonly in solids, more controlled realisations in ion traps have recently been proposed [24]. We extend to the two-spin-boson model as follows: we consider a linear ion trap with the internal levels of a single ion representing each spin, coupled to the collective motion of N ions providing a (finite) bosonic bath. The two-spin-boson Hamiltonian is generated by simultaneously addressing two ions with traveling waves which, in a linear ion trap, gives rise to an Ohmic spectral density $J(\omega) = (\alpha/2)\omega$. The static field Δ is set by the laser-ion Rabi frequency. The strength of the system-bath interaction can be adjusted by varying various experimental parameters such as the laser wavelength and ion mass. We work in the weak coupling regime and therefore set $\alpha = 0.1$ [19]. Addressing the ions in the way described also induces an effective Ising interaction between the two ions due to the polaron representation [24], which nevertheless disappears for a finite lattice with Ohmic spectral density.

Owing to the finite size of the bath, the system evolves as if it were coupled to a continuum only for short times, after which a quantum revival is seen. For example, for $N = 100$ this revival occurs at approximately $2\pi/\omega_t$, where ω_t is the trapping frequency [24]. Hence, to observe both the generation and subsequent decay of the dissipatively-induced entanglement we describe, this period must be larger than both γ_0^{-1} and $(\delta\gamma_0)^{-1}$. Since both γ_0 and δ depend on Δ , this corresponds to a careful choice of Δ . With $\Delta = 25\omega_t$ (set by the Rabi frequency),

we find a revival time $\sim 50\gamma_0^{-1}$. Assuming the wavelength associated with Δ to be approximately $N/(\Delta/\omega_t)$ in units of the ion spacing, we choose to address two neighbouring ions to give $\delta = (\Delta/\omega_t N)^2/2D \approx 0.03$.

Furthermore, the temperature of the bath must be low enough such that the inequality of Eq. (20) is satisfied, allowing a finite level of entanglement to be generated. By requiring $R = 1/2$ we find that the bath must have a temperature in the mK range for typical trapping frequencies of MHz. We conclude that after a timescale $\sim \gamma_0^{-1} = (25\pi\alpha\omega_t)^{-1}$ a concurrence of $C \approx 0.15$ should be generated from the initial state $|\uparrow\downarrow\rangle$ in x , y or z . It will subsequently decay by at least a factor of e^{-1} before the dynamics associated with the finite size of the bath becomes significant.

VIII. SUMMARY

We have shown that the mechanisms normally associated with dissipative processes can lead to long-lived entanglement in *non-interacting, spatially separated* two-qubit systems. We have highlighted two important timescales. The first, shorter timescale γ_0^{-1} is that with which we expect a single qubit to dephase. When a second qubit is introduced close to the first, we find dissipatively-induced entanglement is generated on this short timescale, and further that there is a second larger timescale $(\delta\gamma_0)^{-1}$ on which the induced entanglement decays. Importantly, the influence of both the bath-induced Lamb-shift or a direct spin exchange interaction is still restricted to the original shorter timescale. Hence, the presence of a second qubit within the bath induces coherences in the overall system state that can persist on timescales far larger than either the corresponding single qubit decoherence time, or timescales associated with the influence of direct exchange or the Lamb-shift.

A. Acknowledgements

We thank H. T. Ng for useful discussions. SB thanks the Royal Society and Wolfson Foundation. DPSM, AN and SB are supported by the EPSRC.

-
- [1] M. A. Nielsen and I. L. Chuang, *Quantum Computation and Quantum Information* (Cambridge University Press, 2000).
 - [2] H.-P. Breuer and F. Petruccione, *The Theory of Open Quantum Systems* (Oxford University Press, 2002).
 - [3] T. Yu and J. H. Eberly, Phys. Rev. B **66**, 193306 (2002).
 - [4] D. A. Lidar, I. L. Chuang, and K. B. Whaley, Phys. Rev. Lett. **81**, 2594 (1998).
 - [5] P. Zanardi and M. Rasetti, Phys. Rev. Lett. **79**, 3306

- (1997).
- [6] G. Gordon and G. Kurizki, Phys. Rev. Lett. **97**, 110503 (2006).
- [7] F. F. Fanchini and R. d. J. Napolitano, Phys. Rev. A **76**, 062306 (2007).
- [8] S. Maniscalco, F. Francica, R. L. Zaffino, N. L. Gullo, and F. Plastina, Phys. Rev. Lett. **100**, 090503 (2008).
- [9] B. Kraus and J. I. Cirac, Phys. Rev. A. **63**, 062309 (2001).

- [10] S. D. Barrett and P. Kok, Phys. Rev. A **71**, 060310(R) (2005).
- [11] A. Blais, R. Huang, A. Wallraff, S. M. Girvin, and R. J. Schoelkopf, Phys. Rev. A **69**, 062320 (2004).
- [12] D. Braun, Phys. Rev. Lett. **89**, 277901 (2002).
- [13] F. Benatti, R. Floreanini, and M. Piani, Phys. Rev. Lett. **91**, 070402 (2003).
- [14] D. Solenov, D. Tolkunov, and V. Privman, Phys. Rev. B **75**, 035134 (2007).
- [15] S. W. J. An and H. Luo, Physica A **382**, 753 (2007).
- [16] T. Choi and H. J. Lee, Phys. Rev. A. **76**, 012308 (2007).
- [17] F. Benatti and R. Floreanini, J. Opt. B **7**, S429 (2005).
- [18] T. Zell, F. Queisser, and R. Klesse, Phys. Rev. Lett. p. 160501 (2009).
- [19] A. J. Leggett, S. Chakravarty, A. T. Dorsey, M. Fisher, A. Garg, and W. Zwerger, Rev. Mod. Phys. **59**, 1 (1987).
- [20] M. Dube and P. Stamp, Int. J. Mod. Phys. B **12**, 1191 (1998).
- [21] G. D. Mahan, *Many-Particle Physics* (Plenum, 1990).
- [22] P. Zanardi, Phys. Rev. A **57**, 3276 (1998).
- [23] W. K. Wootters, Phys. Rev. Lett. **80**, 2245 (1998).
- [24] D. Porras, F. Marquardt, J. von Delft, and J. I. Cirac, Phys. Rev. A **78**, 010101(R) (2008).